Available online at www.sciencedirect.com
ScienceDirect
Ceramics International 36 (2010) 1757–1766
CERAMICS INTERNATIONAL
www.elsevier.com/locate/ceramint

Characterization and in vitro-bioactivity of natural hydroxyapatite based bio-glass–ceramics synthesized by thermal plasma processing

C.P. Yoganand [a], V. Selvarajan [a,*], Valeria Cannillo [b], Antonella Sola [b], E. Roumeli [c], O.M. Goudouri [c], K.M. Paraskevopoulos [c], Mahmoud Rouabhia [d]

[a] *Plasma Laboratory, Department of Physics, Bharathiar University, Coimbatore 46, India*
[b] *Dipartimento di Ingegneria dei Materiali e dell'Ambiente, University of Modena and Reggio Emilia, Via Vignolese, 905, 41100 Modena, Italy*
[c] *Department of Physics, Aristotle University of Thessaloniki, 54124 Thessaloniki, Greece*
[d] *Faculté de Médicine Dentaire et Groupe de Recherche en É cologie Buccale, Pavillon de Médecine Dentaire, Local 1728, Université Laval, Quebec City, Quebec, Canada G1K 7P4*

Received 14 September 2009; received in revised form 20 December 2009; accepted 21 February 2010
Available online 24 April 2010

Abstract

Natural bovine hydroxyapatite/SiO_2–CaO–MgO glass–ceramics were produced using the transferred arc plasma (TAP) processing method. Homogeneous mixtures of HA/25 wt% SiO_2–CaO–MgO and HA/50 wt% SiO_2–CaO–MgO batches obtained by dry mixing the respective compositions in a ball mill were processed in argon plasma using the TAP torch at 5 kW for 1, 2 and 3 min, respectively. The synthesized glass–ceramic samples were studied for phase composition, microstructure and bioactivity. The phase study of the synthesized glass–ceramics revealed the formation of calcium phosphate silicate with traces of calcium silicate. The structural study by SEM revealed that the prepared samples possessed smooth glassy surface morphology. The in vitro-bioactivity of the TAP synthesized glass–ceramics was examined in simulated body fluid (SBF). The SBF test results confirmed the development of crystalline carbonated apatite phase after 12 days of immersion. The cytocompatibility was evaluated through human fibroblast cell proliferation. The fibroblasts culture results showed that the sample was non-toxic and promoted cell growth.
© 2010 Elsevier Ltd and Techna Group S.r.l. All rights reserved.

Keywords: D. Glass–ceramics; D. MgO; D. SiO_2; E. Biomedical applications; Transferred arc plasma

1. Introduction

A variety of artificial bone materials, such as metals, polymeric materials, composites and ceramics, are being explored to restore the diseased bones [1–4]. Calcium phosphate ceramics, especially hydroxyapatite HA, are currently used as biomaterials for a variety of applications in both dentistry and orthopedics, because they form a real bond with the surrounding bone tissue when implanted. HA allows specific biological response in the tissue–implant interface, which leads to the formation of bonds between the bone and the material [5–7].

Varieties of bioactive glasses and glass–ceramics have been investigated for tissue engineering applications in bone repair and are successfully used in several clinical applications. Unique properties of bioactive glasses are their ability to convert to hydroxyapatite in body fluids and in aqueous solutions containing calcium and phosphate ions, and the ability to bond directly to bone. The bone bonding properties of bioactive glasses were foremost reported in 1971 by Hench et al. [1,8]. The silicate-based glasses [8] tend to show a higher bioactive behaviour than calcium phosphate materials [4,9,10]. The rapid bioactive behaviour of silica-based glasses has been related to the role of SiO_2 or silicon in their surface reactions and therefore on their in vivo and in vitro behaviour. Since silicon possesses importance in bone formation and mineralization, and the possibility of producing soluble calcium phosphate phases, it is very interesting to study the mixtures of HA and silicate-based glasses [11].

Plasma technology has in recent years emerged as a novel technique for the manufacture of newer and better materials. Plasma technology is an enabling technology, which integrates

* Corresponding author. Tel.: +91 422 2426576; fax: +91 422 2422387.
E-mail address: vselvrjn47@rediffmail.com (V. Selvarajan).

0272-8842/$36.00 © 2010 Elsevier Ltd and Techna Group S.r.l. All rights reserved.
doi:10.1016/j.ceramint.2010.02.048

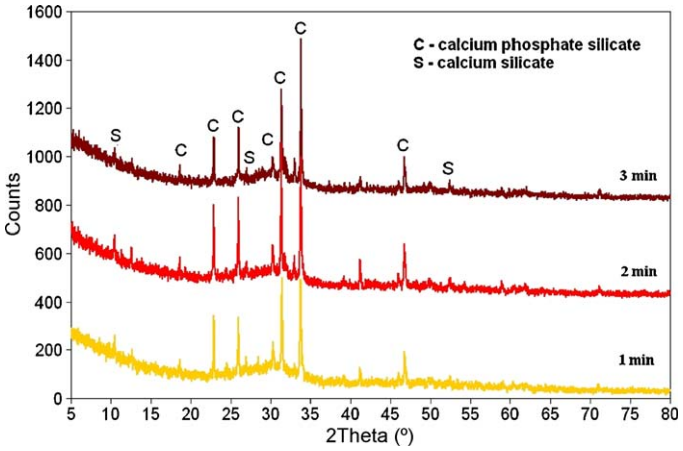

Fig. 1. XRD spectra of HA/50% SiO_2–CaO–MgO glass–ceramics.

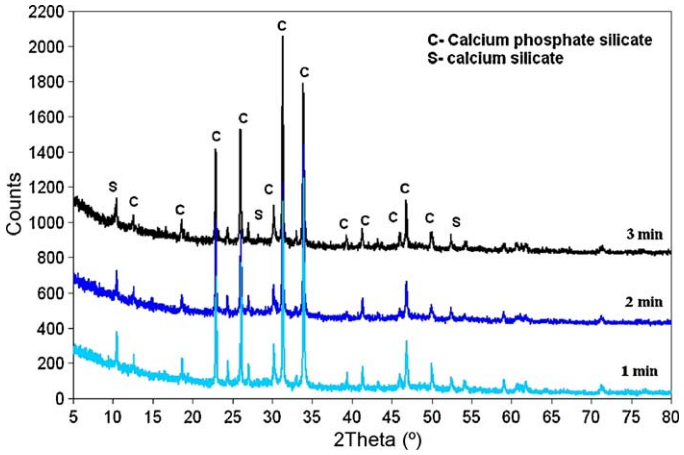

Fig. 2. XRD spectra of HA/25% SiO_2–CaO–MgO glass–ceramics.

processes associated with plasma material interaction with manufacturing, adds value to conventional materials and makes new types of materials and material processing techniques possible [12–16]. In the present study; natural bovine hydroxyapatite/SiO_2–CaO–MgO glass–ceramics were produced using the transferred arc plasma (TAP) melting method.

2. Experimental procedure

2.1. Production of natural bovine HA

The hydroxyapatite used in this study was derived from the natural bovine bones (from the shaft portion of the bovine

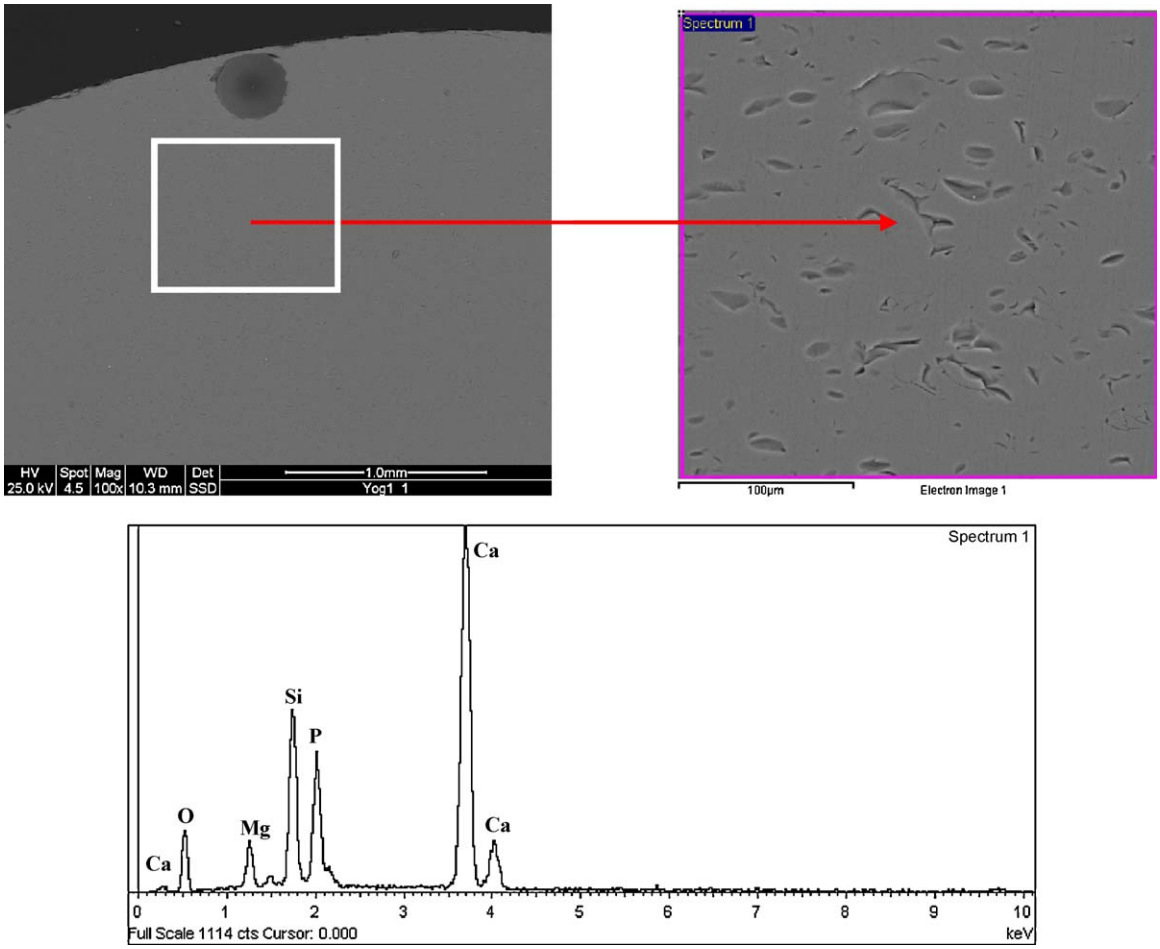

Fig. 3. FESEM with X-EDX image of HA/50% SiO_2–CaO–MgO synthesized for 1 min.

femurs) [17,18]. The bones were irrigated with tap-water and soaked in a 1 wt% concentration of antiseptic solution to prevent contamination of various infectious diseases. Subsequently the bones were reirrigated and deproteinized with reagent grade NaOH treatment. Thereafter the deproteinized bone samples were reirrigated with tap-water again. Then all samples were heated to 850 °C for 5–6 h in a furnace. There after the samples were subjected to grinding with a mechanical grinder. The resulting HA powder was sieved and the particles with an average particle size of 30–40 μm were used for the purpose.

2.2. Plasma synthesis of HA/SiO_2–CaO–MgO glass–ceramics

Initially, SiO_2–CaO–MgO glass–ceramic was obtained by transferred arc plasma (TAP) melting method [19]. Homogeneous mixtures of HA/25 wt% SiO_2–CaO–MgO and HA/50 wt% SiO_2–CaO–MgO batches were obtained by dry mixing the respective compositions for 4 h in a ball mill (In Smart Systems, India). Then the homogeneous mixtures were taken into the anode bed of the dc transferred arc plasma torch. For this experiment, a dc transferred arc plasma torch (Ion Arc Technologies Pvt. Ltd., India) which can be operated at a maximum power of 10 kW was used. The plasma arc is struck between the cathode and the anode by applying a high current arc between them (at an electrode gap about 25 mm) and the desired power level was maintained by controlling the flow rate of the plasma gas and the arc current. The torch was operated at power level of 5 kW. The arc voltage and current was kept maintained at 24 V and 210 A, respectively. Argon at a flow rate of 10 lpm was used as the plasma forming gas. The homogeneous batches were processed for 1, 2 and 3 min, respectively, during which the precursor got melted in the plasma to form glass–ceramic melt. HA/SiO_2–CaO–MgO glass–ceramics were produced by quenching the melts by applying forced air on it. The typical operating parameters are given in Table 1.

Table 1
Typical operating parameters.

Torch type	Transferred arc plasma (TAP) torch
Input power	5 kW
Plasma gas and flow rate	Argon; 10 lpm
Cooling water flow rate	12 lpm
Processing time	1, 2 and 3 min
Quenching medium	Air

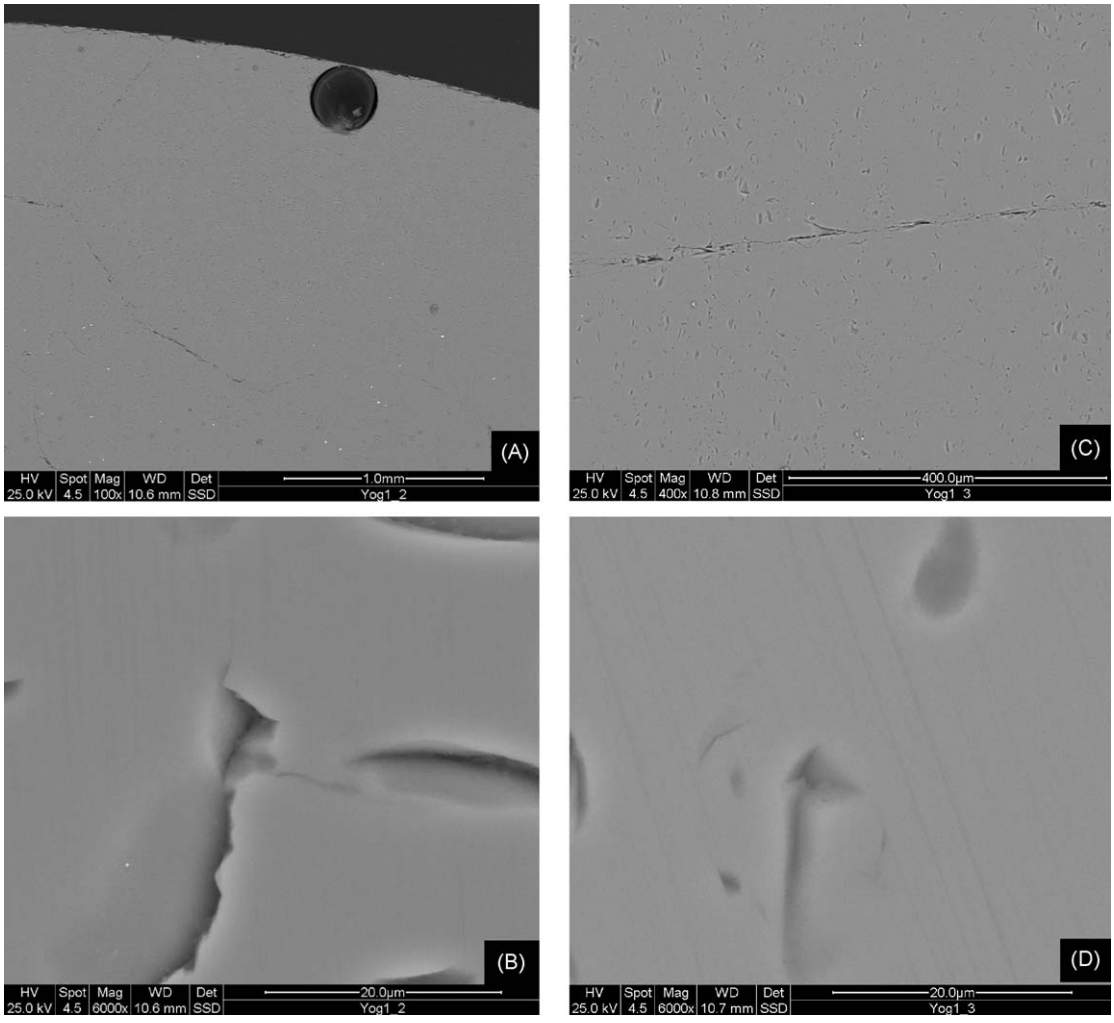

Fig. 4. FESEM images of HA/50% SiO_2–CaO–MgO synthesized for 2 min (a and b) and for 3 min (c and d).

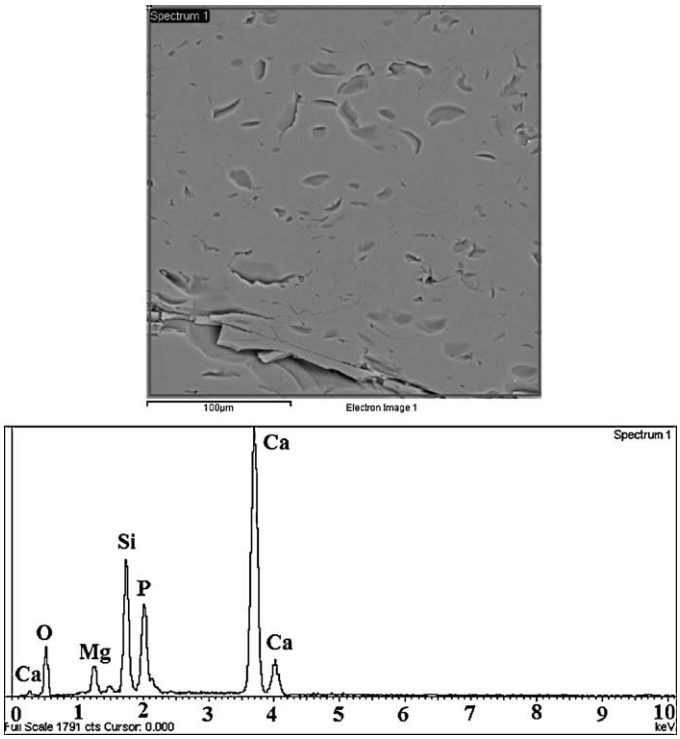

Fig. 5. FESEM image with X-EDX of HA/50% SiO_2–CaO–MgO synthesized for 3 min.

2.3. Phase and microstructural characterization

The synthesized glass–ceramic samples were studied for phase composition and microstructure using energy dispersive X-ray spectral analysis and scanning electron microscopy. The observation was carried out using an ESEM Quanta200-FEI, worked in high vacuum mode. The phase composition of the glass–ceramic samples was furthermore studied by X-ray diffraction analysis. The spectra were acquired using an X'Pert PRO PANAlytical diffractometer, working with Cu Kα radiation ($2\theta = 5–80^\circ$). The micro-hardness and density measurements were carried out for the TAP synthesized glass–ceramic samples. The porosity was determined by using Archimedean porosimetry.

2.4. In vitro-bioactivity analysis

The bioactivity of glass–ceramic samples was examined by in vitro procedures involving dissolution in aqueous media i.e. Simulated body fluid (SBF), like c-SBF, which was prepared as described by Ohtsuki et al. [20]. In the process, 75 mg powder of the glass–ceramic with average particle size of 200 μm was immersed in 50 ml c-SBF for several days. After filtration, the powders were rinsed with distilled water, dried and a quantity of 0.003 g with 0.2 g of KBr was pressed each time in a vacuum press at 7 t in order to produce a pellet with 13 mm diameter and 0.8 mm thickness. The pellets were then characterized with Fourier transform infrared spectroscopy (FTIR). The remaining reacted powders were carbon coated for scanning electron microscopy and energy dispersive spectroscopic analysis. The FTIR spectra were collected using a Bruker IFS113v FTIR spectrometer, in transmission mode in MIR region (400–4000 cm^{-1}) with a resolution of 4 cm^{-1}.

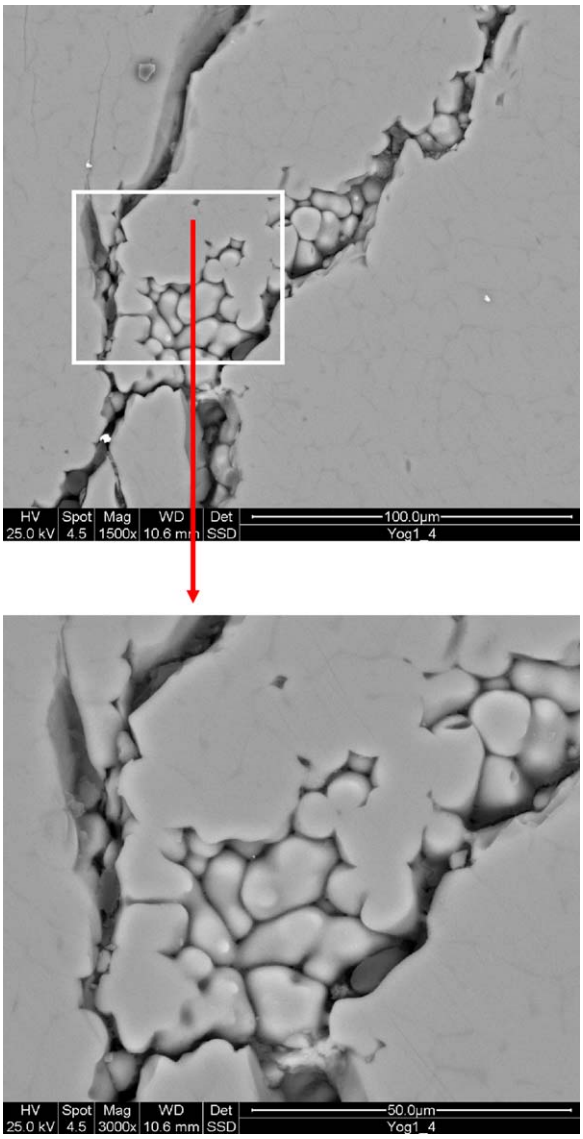

Fig. 6. FESEM image of HA/25% SiO_2–CaO–MgO synthesized for 1 min showing granulous microstructure at the matrix.

2.5. Cytocompatibility analysis

Normal human skin fibroblasts were grown in 75 cm^2 cell culture flasks (Falcon, Becton-Dickinson, Cockeysville, MD, USA) in Dulbecco's modified Eagle's medium (DMEM, Invitrogen Life Technologies, Burlington, ON, Canada) with 10% fetal calf serum (FCS, Invitrogen Life Technologies), 100 IU/ml penicillin G, 25 μg/ml streptomycin and 0.5 μg/ml fungizone (Sigma–Aldrich Canada, Ltd.). The cultured cells were then incubated at 37 °C in 98% humidity, and 5% CO_2. Cell culture medium was changed every 2–3 days. When the cultures reached 90% confluence, the cells were detached from the flasks using a 0.05% trypsin–0.1% EDTA solution, washed twice, and were used to evaluate their adhesion and growth onto the synthesized glass–ceramic. Fibroblasts were seeded into 24

well plates. Each well contains small pieces of the glass–ceramic. Materials were sterilized using 2 mn × 30 mn incubation in 70% ethanol. Following three washes with sterile DMEM, each well was seeded with 10^3 fibroblasts and cultured for 24 and 48 h. At the end of each incubating period fibroblasts that adhered to the materials were visualized using Hoechst staining. To do so, cells on the materials were fixed with 75% methanol (EMD Chemicals Inc., Gibbstown, NJ, USA) and 25% glacial acetic acid (Laboratoire MAT Inc.) solution (v/v) for 5 mn. Following 2 washes with PBS, each well was then supplemented with 0.5 ml Hoechst dye (1 μg/ml) (Molecular Probes, Eugene, OR, USA) and the specimens were incubated for 15 min at room temperature before being extensively washed with distilled water, observed under an epifluorescence light microscope (Axiophot, Zeiss, Oberkochen, Germany), and photographed using a digital camera.

3. Results and discussion

In transferred arc plasma melting, the plasma arc strikes between the anode wall (melting bed) and the cathode tip of the TAP torch and then randomly spread to all parts of the melting bed. Glass–ceramics were produced by melting the precursor material in the melting bed and solidification (after cut of the plasma arc). The quenching process was carried out by applying forced air on the glass–ceramic melt.

3.1. X-ray diffraction (XRD) analysis

The X-ray diffraction spectra of TAP processed HA/50 wt% SiO_2–CaO–MgO glass–ceramics (Fig. 1) with high nominal content of glass and that of HA/25 wt% SiO_2–CaO–MgO glass–ceramics (Fig. 2) with low nominal content of glass were observed to be much similar. HA/50 wt% SiO_2–CaO–MgO samples exhibited more amorphous phase than HA/25 wt% SiO_2–CaO–MgO samples as observed from the trend of the background in the XRD spectra, and this is coherent with the nominal content of glass. Regardless of the nominal composition and the processing parameters, the peaks observed were all due to complex calcium phosphate silicate. Minor peaks were found ascribed to calcium silicon. The formation of complex calcium phosphate silicate may be attributed to the combination of elements present in bovine HA and the SiO_2–CaO–MgO glass–ceramic as a result of melting during TAP processing. Only in the spectra of HA/50 wt% SiO_2–2CaO–MgO samples synthesized for 2 and 3 min some traces of HA were detected, but the identification was uncertain due to the poor intensity of peaks.

3.2. Field emission scanning electron microscopy (FESEM) and energy dispersive X-ray (X-EDX) analysis

Apart from the peripheral areas of the cross-section of TAP processed HA/50 wt% SiO_2–CaO–MgO for 1, 2 and 3 min the microstructure was found to be basically uniform (Figs. 3–5). HA/50 wt% SiO_2–CaO–MgO glass–ceramic synthesized for 1 min showed a two-phase microstructure (light-grey areas surrounded by dark-grey matrix) in the marginal areas of cross-section, wherein the pores were preferentially located. According to X-EDX analysis, light-grey areas were found to be richer in Mg and Si than dark-grey areas which in turn are richer in P. This implies that the light-grey areas were originated by glass, while the dark-grey areas were derived from HA. However, even if the relative amounts were different, the elements such as O, Mg, Si, P, and Ca were detected in both areas. In the core of the sample, the microstructure was found to be extremely homogeneous. In case of HA/50 wt% SiO_2–CaO–MgO glass–ceramic synthesized for 2 min the marginal areas of the cross-section was still irregular; moreover cracks run across the sample which could have been generated during sample preparation. In the core of the sample the microstructure is extremely uniform. The chemical composition was analogous to that of HA/50 wt% SiO_2–CaO–MgO synthesized for 1 min. The microstructure of 3 min synthesized HA/50 wt% SiO_2–CaO–MgO glass–ceramic was quite similar to HA/50 wt% SiO_2–CaO–MgO synthesized for 2 min, with very defective borders and a compact, homogeneous core. In the core of the sample, the microstructure is very uniform with the same chemical composition.

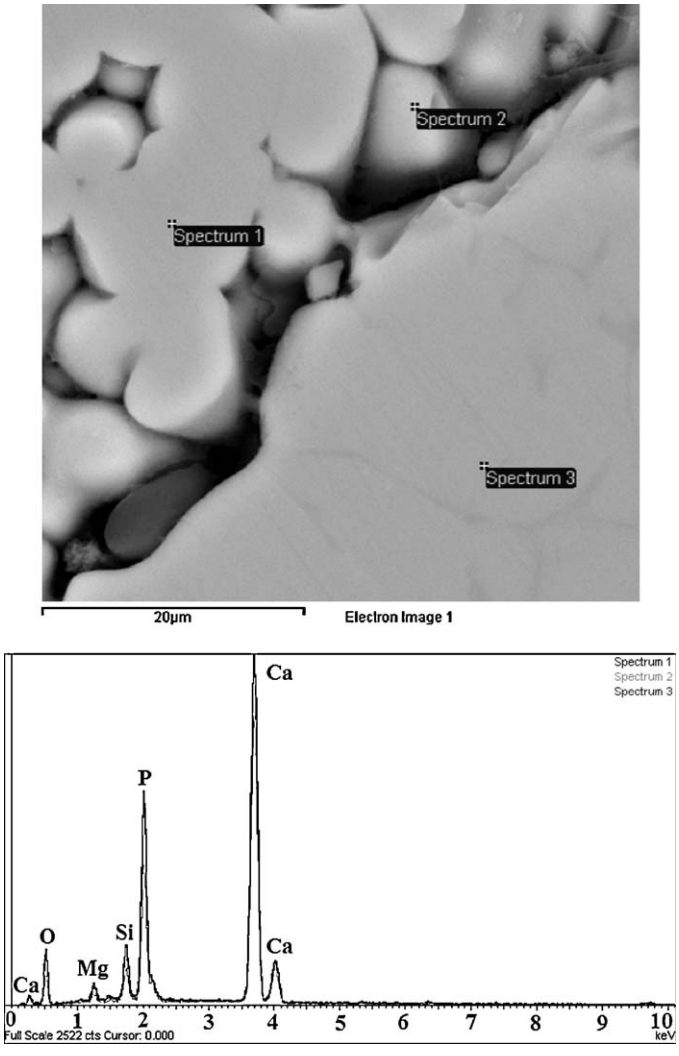

Fig. 7. FESEM image with X-EDX of HA/25% SiO_2–CaO–MgO synthesized for 1 min.

The microstructure of HA/25 wt% SiO_2–CaO–MgO glass–ceramic synthesized for 1 min was found to be interesting because of the observed cracks and pores making it to appear as in ''granulous'' microstructure (Figs. 6 and 7). This indicated that the starting powders had some extent preserved their original shape. The cross-section showed two different phases: light-grey rounded particles surrounded by darker matrix. It could be suggested that the light areas are the section of the round particles visible in the pores. The dark areas were found to be richer in Mg and Si than the light-grey areas, which in turn were richer in P and Ca. The difference between light-grey particles and dark-grey matrix was even visible (perhaps it is even more evident) in 2 min synthesized HA/25 wt% SiO_2–CaO–MgO glass–ceramic samples (Fig. 8). The chemical compositions of the two phases were similar to HA/25 wt% SiO_2–CaO–MgO sample synthesized for 1 min. In case of HA/25 wt% SiO_2–CaO–MgO glass–ceramic synthesized for 3 min the marginal areas of the cross-section were found to be particularly rich in impurities and defects (pores and inclusions). The microstructure in the core of the 3 min sample (Fig. 9) was quite similar to that of HA/25 wt% SiO_2–CaO–MgO synthesized for 2 min, with cracks (but no granulous features) and dark/light areas. The compositions of the two phases were similar to those of HA/25 wt% SiO_2–CaO–MgO synthesized for 2 min.

3.3. Microstructure and mechanical properties (density, hardness and porosity)

The average density values of the HA/50% SiO_2–CaO–MgO samples were found to be 2.78, 2.82 and 2.88 g/cm^3 for 1, 2 and 3 min, respectively. For HA/25% SiO_2–CaO–MgO samples the average density values were 2.68, 2.72 and 2.77 g/cm^3 for 1, 2 and 3 min synthesis. The average porosity measured by Archimedes method was found to be 12.13%, 9.66% and 7.99% for 1, 2 and 3 min synthesized HA/50% SiO_2–CaO–MgO samples. In case of HA/25% SiO_2–CaO–MgO the average porosity values were 12.13%, 9.66% and 7.99% for 1, 2 and 3 min synthesized samples. The decrease in porosity for the 3 min synthesized samples in both the cases may be due to the

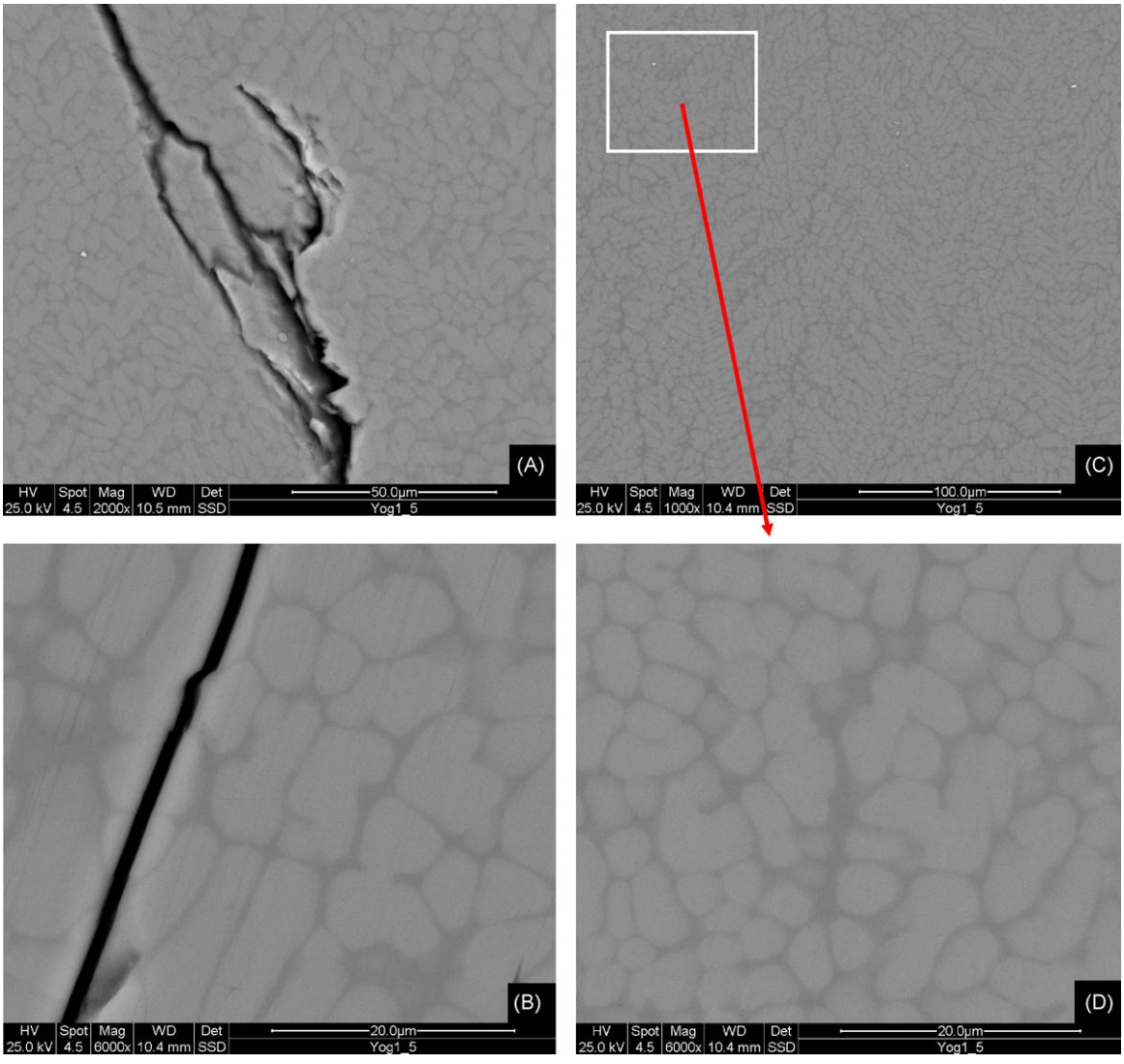

Fig. 8. FESEM images of HA/25% SiO_2–CaO–MgO synthesized for 2 min.

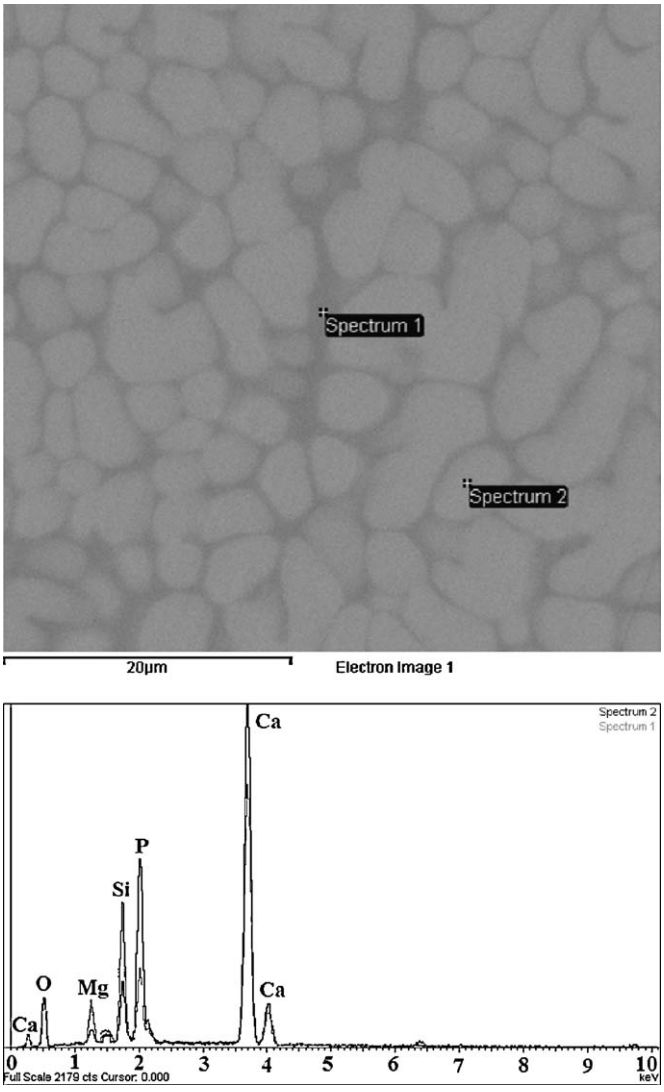

Fig. 9. FESEM image with X-EDX of HA/25% SiO_2–CaO–MgO synthesized for 3 min.

reason that higher treatment time offers higher thermal treatment with higher melting rate; this in turn produces glass–ceramics with less porosity and improved hardness. The average hardness values of the HA/SiO_2–CaO–MgO glass–ceramics are shown in Fig. 10.

3.4. Bioactivity of TAP synthesized HA/SiO_2–CaO–MgO glass–ceramics

3.4.1. Simulated body fluid (SBF) test results

Fig. 11a and b shows the FTIR spectra of HA/SiO_2–CaO–MgO glass–ceramics (synthesized for 3 min) before and after the immersion in c-SBF for 0–15 days. After 3 day of soaking, the spectrum of the glass–ceramics revealed the formation of an amorphous Ca–P phase, as it can be observed by the formation of the broad peaks at 1000–1100 and 570 cm^{-1} that are attributed to the stretching and bending vibrational mode of PO group. After 9 days in c-SBF, the IR spectrum of the glass–ceramics was analogous to that observed after 3 day. However, after 12 days a double peak at

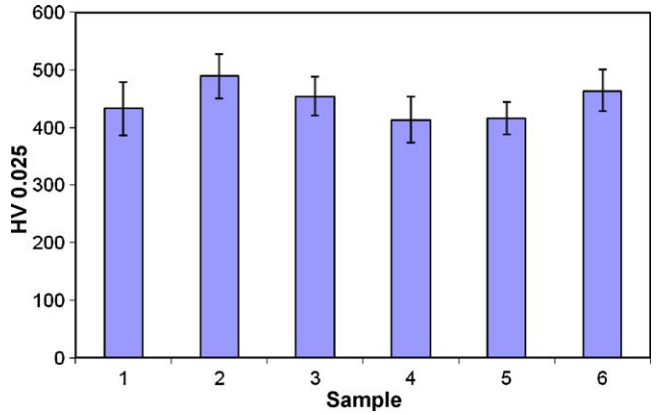

Fig. 10. Hardness values of the HA/glass–ceramics synthesized for 1, 2 and 3 min (1, 2 and 3: HA/50% SiO_2–CaO–MgO synthesized for 1, 2 and 3 min; 4, 5 and 6: HA/25% SiO_2–CaO–MgO synthesized for 1, 2 and 3 min, respectively).

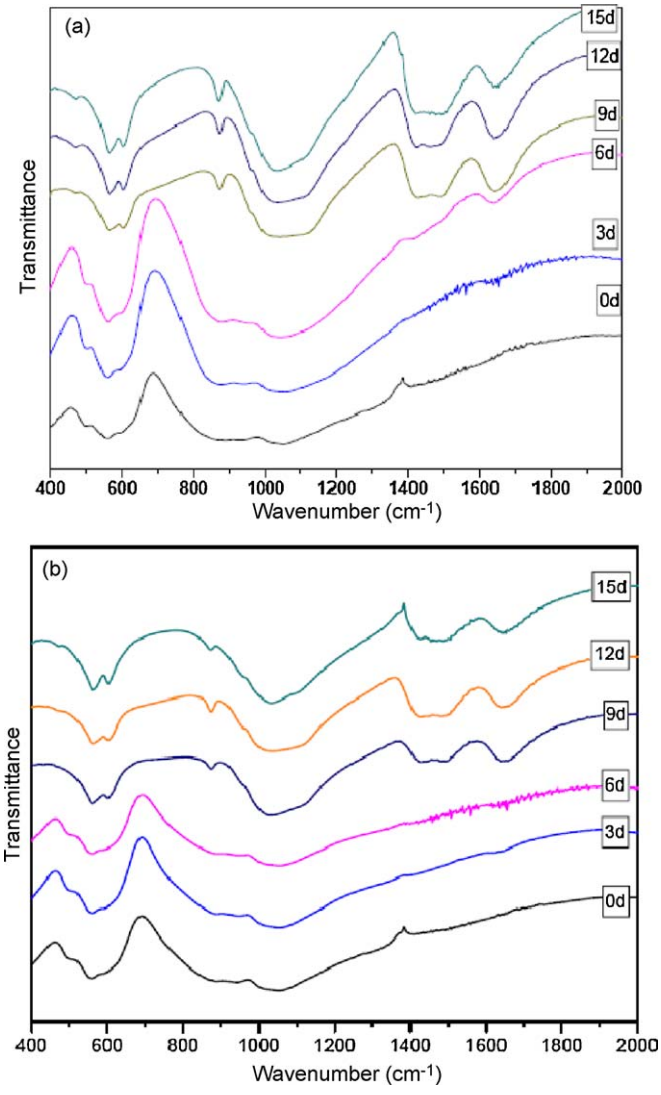

Fig. 11. FTIR spectra of (a) HA/50% SiO_2–CaO–MgO (b) HA/25% SiO_2–CaO–MgO before and after the immersion in c-SBF, for 0–15 days.

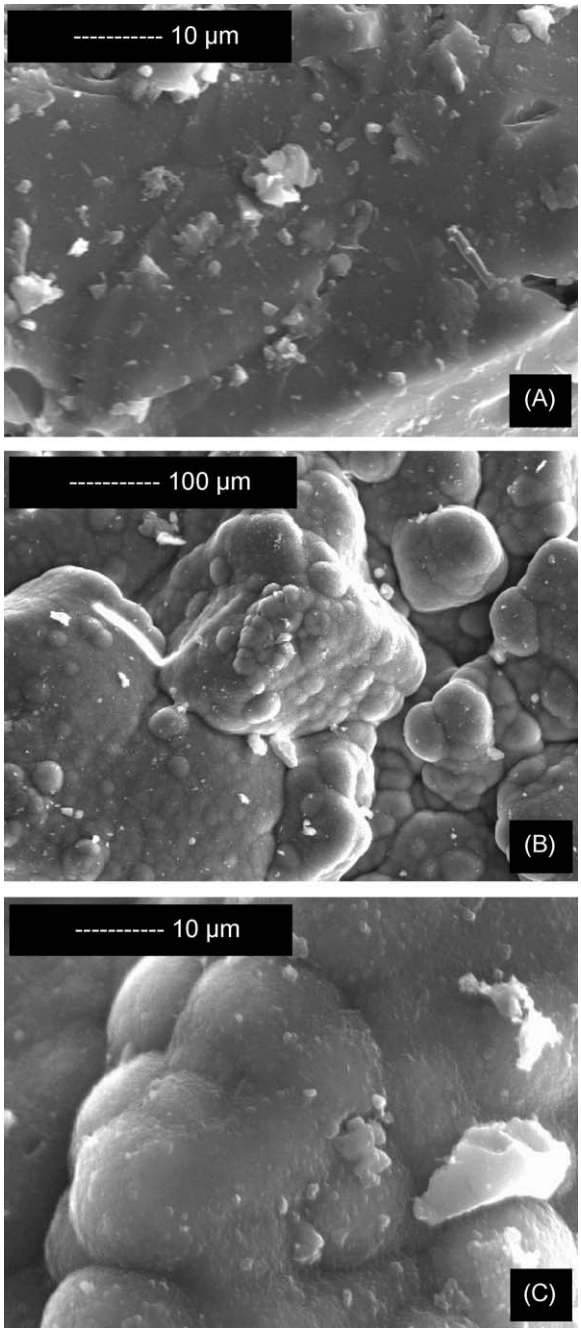

Fig. 12. SEM microphotographs of HA/50% SiO_2–CaO–MgO (a) before and (b and c) after immersion in c-SBF for 15 days.

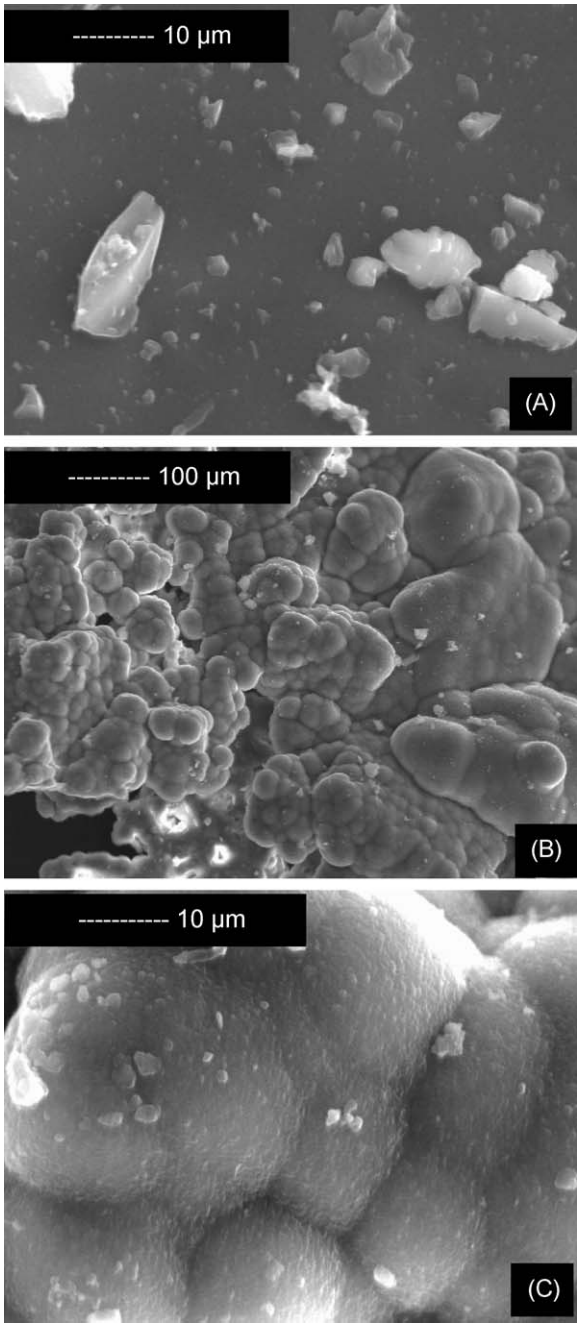

Fig. 13. SEM microphotographs of HA/25% SiO_2–CaO–MgO (a) before and (b and c) after immersion in c-SBF for 15 days.

568 and 602 cm^{-1} got developed, that attributed to the bending of P–O mode and proved the development of a crystalline phase of HCAp. These findings are in accordance with SEM microphotographs that are presented in Figs. 12 and 13 and revealed the development of an amorphous layer of apatite on the whole surface of all grains, while EDX analysis revealed a mean molar Ca/P ratio ranging between 1.6 and 2.6. The FTIR spectra of both composite materials after 9 days of immersion revealed the formation of an amorphous Ca–P phase. However, after 9 days of immersion the spectra of both composite samples correspond to that of pure carbonate hydroxyapatite. In details the broad peak at 1100–1000 cm^{-1} and the double peak at 604 and 560 cm^{-1} are attributed to the stretching and bending vibrational mode of PO group. Additionally, the double peak at 1500 and 870 cm^{-1} is attributed to CO_3 group of HCAp. On the surface of the grains of both the composite samples immersed for 9 days in c-SBF, SEM microphotographs reveal the development of a dense HCAp layer with spherulitic appearance. EDX analysis revealed a molar Ca/P ratio of about 1.68, while the peaks attributed to Si and Mg from the substrate have almost disappeared, suggesting a

Table 2
EDX elemental analysis of the HA/50% SiO_2–CaO–MgO after immersion in c-SBF for 15 days.

Element	Element%	Atomic%
O	59.98	76.18
Na	0.17	0.15
Mg	0.84	0.72
Al	0.13	0.10
Si	0.46	0.34
P	13.96	9.32
S	0.31	0.20
Cl	0.37	0.22
K	0.11	0.06
Ca	24.66	12.72

thick and well-formed apatite layer. The EDX elemental analysis of both the type of glass–ceramic after 15 days immersion in SBF are given in Tables 2 and 3.

SEM microphotographs of the HA/SiO_2–CaO–MgO samples (Figs. 12 and 13) revealed that the surfaces of glass–ceramics materials before immersion in c-SBF were smoother and vitrified in nature, whereas the surfaces of the samples immersed in c-SBF were rough and fully covered by HCAp granules due to the interaction of the surface of the glass–ceramic materials with the c-SBF solution. The FTIR results were in good agreement with SEM images and indicated the development of an amorphous layer of apatite on the whole surface of all grains. It is clear that, when immersed in SBF, precipitation takes place on the surfaces. The two composites seem to have the same bioactive behaviour, even though from SEM microphotographs it is indicated that the HCAp layer on the grains of HA/25% SiO_2–CaO–MgO composite is thicker and better formed. However, the thickness and the morphology of the apatite layer on both composites are astounding.

3.4.2. Cell culture results

Figs. 14a and 15a show the glass–ceramic surfaces (synthesized for 3 min) after 24 h being seeded by human fibroblast cells. Figs.14b and 15b show that the fibroblasts cells get firmly attached on the glass–ceramic surface after 48 h. The UV epifluorescence microscopic images revealed

Table 3
EDX elemental analysis of the HA/25% SiO_2–CaO–MgO after immersion in c-SBF for 15 days.

Element	Element%	Atomic%
O	43.57	63.62
Na	0.29	0.30
Mg	0.75	0.72
Al	0.10	0.08
Si	0.16	0.13
P	17.03	12.85
S	0.36	0.26
Cl	0.38	0.25
K	0.04	0.02
Ca	32.32	21.76

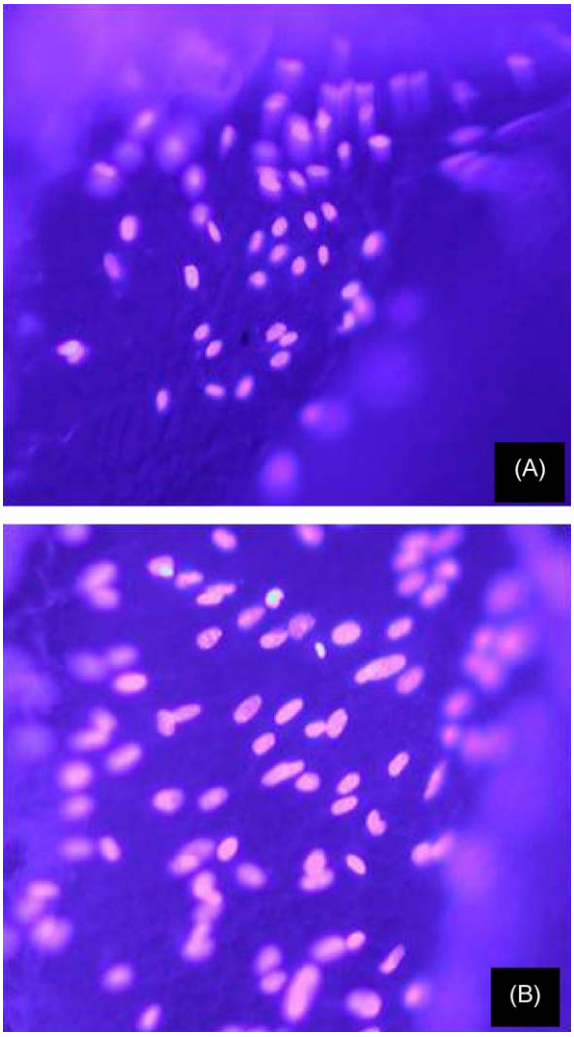

Fig. 14. Human fibroblast cultures on HA/50% SiO_2–CaO–MgO at (a) 24 h and (b) 48 h.

that the seeded human fibroblasts cells spread well and the pseudopods were clearly seen, indicating good livelihood. The samples were non-toxic for in vitro fibroblast cultures. The cells spread throughout the material. Indeed, Hoechst staining revealed that fibroblasts adhere and exhibited a normal elongated and spread-out morphology as those cultured on cell culture surfaces. Of great interest the glass–ceramic samples seemed to highly promote fibroblast adhesion. The fibroblasts density as visualized by cell staining showed that these cells grow well after seeding onto the materials. In general, these results showed that the glass–ceramic sample were non-toxic to human fibroblasts and promote cell growth.

Overall in this work, the c-SBF immersion results confirmed the development of crystalline phase of HCAp. The human fibroblasts culture test revealed that the seeded human fibroblasts cells spread well and the pseudopods were clearly seen, indicating the materials bioactivity. These results clearly indicate that the plasma synthesized HA/SiO_2–CaO–MgO glass–ceramic samples possess good bioactivity.

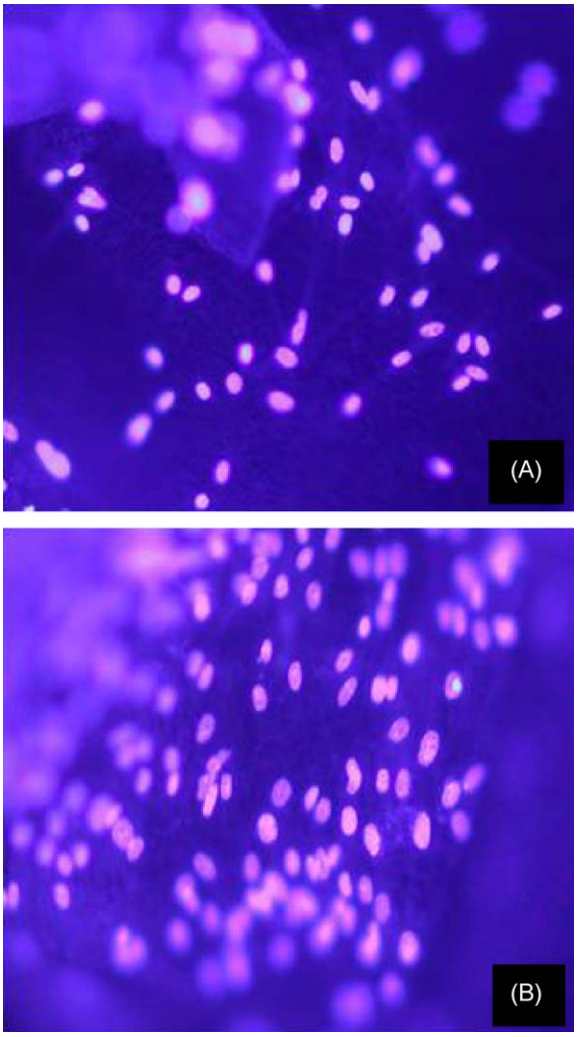

Fig. 15. Human fibroblast cultures on HA/25% SiO_2–CaO–MgO at (a) 24 h and (b) 48 h.

4. Conclusion

The TAP synthesized natural bovine hydroxyapatite based glass–ceramic samples were studied for phase composition and microstructure. The bioactivity of glass–ceramic material was examined by involving the dissolution in simulated body fluid (SBF). The SBF immersion results confirmed the development of crystalline HCAp phase. The human fibroblasts culture results showed that the sample was non-toxic and promote cell growth. From the study, it is possible to suggest that the transferred arc plasma synthesized HA/SiO_2–CaO–MgO glass–ceramics may possibly be of interest in biomedical applications.

Acknowledgements

The authors acknowledge Mr. Janarthanan Nair (Ion Arc Technologies Pvt. Ltd., Coimbatore) for providing torch facilities. One of the authors Mr. C.P. Yoganand acknowledges the grant of seniour research fellowship by CSIR, Government of India.

References

[1] L.L. Hench, Bioceramics: from concept to clinic, J. Am. Ceram. Soc. 74 (1991) 1485–1510.
[2] D.W. Hutmacher, Polymeric scaffolds in tissue engineering bone and cartilage, Biomaterials 21 (2000) 2529–2543.
[3] M. Niinomi, Fatigue characteristics of bioactive glass–ceramic-coated Ti–29Nb–13Ta–4.6Zr for biomedical application, Biomaterials 25 (2004) 3369–3376.
[4] C.E. Wen, W. Xu, W.Y. Hu, P.D. Hodgson, Hydroxyapatite/titania sol–gel coatings on titanium–zirconium alloy for biomedical applications, Acta Biomater. 3 (2007) 403–410.
[5] S.F. Hulbert, L.L. Hench, D. Forbers, L.S. Bowman, History of bioceramics, Ceram. Int. 8 (1982) 131–140.
[6] P. Ducheyne, S. Radin, L. King, The effect of calcium phosphate ceramic composition and structure on in vitro behavior, J. Biomed. Mater. Res. 27 (1993) 25–34.
[7] E. Schepers, M. de Clercq, P. Ducheyne, R. Kempeneers, Bioactive glass particulate material as a filler for bone lesions, J. Oral. Rehab. 18 (1991) 439–452.
[8] L.L. Hench, R.J. Splinter, W.C. Allen, T.J. Greenlee Jr., Bonding mechanisms at the interface of ceramic prosthetic materials, J. Biomed. Mater. Res. 2 (1971) 117–141.
[9] M. Vallet-Regí, C.V. Ragel, A.J. Salinas, Glasses with medical applications, Eur. J. Inorg. Chem. 6 (2003) 1029–1042.
[10] H. Oonishi, L.L. Hench, J. Wilson, F. Sugihara, E. Tsuji, T. Matsuura Yamamotto, S. Mizokawa, Quantitative comparison of bone growth behavior in granules of bioglass-A-W glass–ceramic, and hydroxyapatite, J. Biomed. Mater. Res. 51 (2000) 37–46.
[11] S. Padilla, J. Román, S. Sánchez-Salcedo, M. Vallet-Regí, Hydroxyapatite/SiO_2–CaO–P_2O_5 glass materials: in vitro bioactivity and biocompatibility, Acta Biomater. 2 (2006) 331–342.
[12] B. Gross, B. Grycz, K. Miklossy, Plasma Technology, Iliffe Books, London, 1969.
[13] S.V. Dresvin, Physics and Technology of Low Temperature Plasmas, Atomizdat, Moscow, 1972.
[14] E. Pfender, Gaseous Electronics, Academic Press, New York, 1978.
[15] V. Dembovsky, Plasma Metallurgy—The Principles, Elsevier, Amsterdam, 1985.
[16] O.P. Solonenko, M.F. Zhukov, Thermal Plasma and New Materials Technology, Cambridge Interscience Publishing, Cambridge, 1995.
[17] G. Goller, F.N. Oktar, F.N. Ozyegin, L.S. Kayali, E.S. Demirkesen, Plasma-sprayed human bone-derived hydroxyapatite coatings: effective and reliable, Mat. Lett. 58 (2004) 2599–2609.
[18] R. Murugan, S. Ramakrishna, Porous bovine hydroxyapatite for drug delivery, J. Appl. Biomater. Biomech. 2 (2005) 93–97.
[19] M.L. Ernest, C.R. Robbins, H.F. McMurdie, Phase Diagrams for Ceramists, American Ceramic Society Inc., Westerwille, OH, 1994.
[20] C. Ohtsuki, H. Kushitani, T. Kokubo, S. Kotani, T. Yamamuro, Apatite formation on the surface of ceravital-type glass–ceramic in the body, J. Biomed. Mater. Res. 25 (1991) 1363–1370.